

# MAE 4620 Final Report

## Autonomous Robot Team

### **Team Members:**

Hannah Clark  
Erin Dubas  
Daniel Helmus  
Charles Kellas  
Cynthia Okoye  
Connor Wynkoop

### **Date of Completion:**

05/12/2021

## Introduction

### The Issue at Hand

The Coronavirus disease of 2019 (Covid-19) has been a worldwide viral pandemic, the seriousness of which has not been seen for a century (Walsh, 2020). According to the Centers for Disease Control and Prevention (CDC) website (<https://covid.cdc.gov/>) 32 million cases and 570,000 deaths have been reported in the United States as of April 28, 2021. The disease is mostly spread through direct contact with those who are infected and indirect contact with surfaces that have previously been exposed to the virus (“What to do if you were potentially exposed to coronavirus disease (COVID-19)?,” 2021). Because carriers are not guaranteed to exhibit symptoms, the difficulties of tracking and controlling the spread of the disease are increased (Edwards, 2020). In particular, symptomless carriers can compromise surfaces exposed to healthy members of the public, on which the virus can remain infectious for up to three days (“How coronavirus spreads,” 2020; Mortensen, 2020). This motivates accelerated development of improved means, specifically disinfection, to address this issue in mass gathering environments such as hospitals (Hu, Zhong, Li, Tan, & He, 2020). To help slow the spread, a semi-autonomous robot can be used to reduce spread via contaminated surfaces and aerosolized water droplets (Cresswell & Sheikh, 2020).

### Previous Attempts at Resolution

Disinfection of surfaces and aerosolized water droplets has been in use for some time, and multiple solutions with varying degrees of complexity have been developed, including many robotics based technologies (Blancou, 1995; Keutel, 2020). Some perform disinfection using aerosols while others take advantage of light-based technologies. For example, the Xenex LightStrike UV-C (ultraviolet-C) robot has been proven in 2020 by Schaffzin, Wilhite, Li, and Finney to decrease hospital acquired infections by 16.2% following implementation and regular use of 2 Xenex robots (p. 904). However, this specific robot must be placed in each position by a technician and operated remotely. As early as February 2020, a Shanghai robotics company TMiRob produced 30 disinfection robots utilizing a hydrogen peroxide sprayer and nine ultraviolet lamps each. They are used in Wuhan’s major coronavirus hospital wards, operating theaters, ICUs, consultation rooms and pathology labs (“Intelligent Sterilization Robot,” n.d.). The robots are able to avoid obstacles and disinfect surfaces autonomously or by navigating via a pre-uploaded floor plan map, and the use of a sprayer adds another method of deactivating microorganisms.

The UVD Robot developed by Blue Ocean Robotics in Sweden provides a more autonomous solution than the above examples and uses ultraviolet light (UV), specifically the C band of the light, to disinfect surfaces (UVD Robots. n.d.). The robot enters a room, maps the space and uses long vertical tube lamps of UV light to sanitize surfaces. This method allows for disinfection with minimal exposure to humans and can disinfect 500 square meters in less than 30 minutes (“UVD Robots,” n.d.). However, when the robot maps spaces, it creates a two-dimensional map producing inconsistency in the degree of disinfection achieved on non-vertical surfaces. In the case of both designs, the lights are statically fixed to the robot, cannot move closer to surfaces without repositioning the robot and may not disinfect horizontal surfaces effectively. Solutions with an increased degree of autonomy have also been explored by aerosol systems, including a simulated robot developed by researchers in Malaysia and Indonesia

that is based on internet-of-things technology and disinfects using a mixture of bleach and water (Mohammed et al., 2020). When simulated, the robot could achieve the purification of large zones in less time than it would have taken a human and with little required human interaction. However, it required manual setting of joint angles and wheel speeds and had limited sensors and sensor programming resulting in difficulty navigating obstacles. Though its theoretical performance has been evaluated, it is not an applied example of success. Many robots are similar to the prior designs attempting to achieve related results while incorporating further improvements and complexity. One such variation was developed by Conte et. al.. One of the main advantages of their solution was the use of a movable light source to disinfect non-vertical surfaces more effectively, using a lamp mounted on a robotic arm. A sensor mounted on the end of the arm allowed for precise positioning of the lamp for disinfection. Further advantages include semi-autonomous operation over Long-Term-Evolution (LTE) communication.

### Aims of the Authors

The aim of this work is to build a robot that will disinfect surfaces and aerosolized water droplets using ultraviolet-C light. The robot will be controlled wirelessly, with the operator using a map of the robot's surroundings as well as a camera. The robot must have sufficient mobility and be safe to operate in a dynamic and complex indoor environment.

### Plans of the Authors

The design and development of the robot is detailed below, paralleling Karl T. Ulrich and Steven Eppingers novel, *Product Design and Development*, and starting with an exploration into past work (1999). Informed by knowledge of previous efforts, various solutions are considered before one is selected. After considering many combinations of solutions for several problems, each aspect is weighted, and given a numerical score to determine the best combination for this robot. After this, more specific details are fleshed out, such as overall design and some individual parts, to obtain a concrete idea of how the finished product will perform. The design process is iterative, with some parts of the robot going through several changes. This paper follows these steps with an explanation of the total final design, with the rationale behind each decision explained. Next, after showing results in order to validate the robot, a manual is used to explain the operation of the robot, possible failures and limitations, troubleshooting, and assembly of the system. Finally, the direction of future work is discussed.

## **Previous Design and Essential Information**

Following the outbreak of Covid-19 in the spring of 2020, a team at the University of Virginia (UVA) designed its own decontamination robot to combat the virus. This robot was created by Dean Conte, Spencer Leamy and Tomonari Furukawa. It was built as a hybrid which modified a preexisting unmanned ground vehicle's (UGV) rectangular body to include 7 UV-C light tubes around the body, a camera, and a robotic arm as pictured below. The design uses UV-C lights to disinfect surfaces to a 99.99% sterilization and removes any error associated with a human disinfection method. These lights are placed around the robot with one on the robot's arm, two on the bottom of the robot and two on either side of its body. One of the novelties in this design lies in the implementation of the robotic arm. The robot arm allows this robot to disinfect surfaces beyond the line of sight which is a capability not found in other disinfection

robots. The arm operates with 6 degrees of freedom, allowing it to have a wide range of motion and makes it capable of reaching obstructed surfaces (Conte, D., Leamy, S., Tomonari, F.).

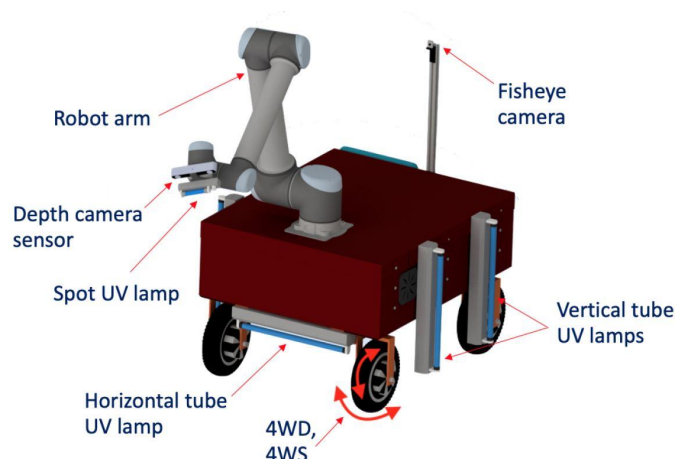


Figure 1. DINGO robot design spring 2020

Many components of this robot provide advantages in its use for disinfection. One such notable novelty is the robot's mapping system. The robot is semi-autonomous and uses a “coarse” and “fine” map in a two step process. First, the robot drives around a room forming the “coarse” 3D map which allows it to generate a map that includes surfaces past the line of sight. From this, an operator is able to determine the path a robot should take to disinfect all surfaces. Next, the robot is guided around the room again where it creates a “fine” map which keeps track of which surfaces have been disinfected. When the robot determines a surface is not vertical, it switches from disinfecting with the vertical tubes around its body to using the robotic arm. This is important because it allows the robot to orient the incident light parallel to a surface, maximizing the power of light hitting the surface. Another important component of this robot is its use of Long-Term Evolution (LTE) for communication. This allows the robot to communicate reliably without interfering with any networks nearby. This is especially crucial in a hospital setting, where this robot would likely be used, because its connection would not interfere with any life saving hospital equipment, nor would the robot's performance be impacted by poor connection (Conte, D., Leamy, S., Tomonari, F.).

Coronavirus can live on surfaces for anywhere from a few hours to a few days. Because of this, it is important to understand which surfaces in a room pose the greatest risk of infection. According to the Centers for Disease Control and Prevention, surfaces are divided into three levels of risk: critical, semi-critical and noncritical. Critical surfaces are exposed to sterile areas of the body and require disinfection or sterilization and pose the greatest risk. Semi-critical surfaces are exposed to human skin while non-critical surfaces are touched by people indirectly and both require disinfection but not sterilization. A study was conducted which looked at the most contaminated surfaces in a hospital room that had been exposed to a bacteria endemic and outbreak (Mitchell, 2020). It determined that the most touched surfaces include bed rails, bed surfaces, over bed tables, and door handles which range from 18 inches to 48 inches off the ground as shown in more detail below. These surfaces are the most important to disinfect and can help to aid in a more well suited design for light placement on the robot.



Table 1. Highest touch surfaces in patient room

<b>Highest Touch Surfaces in Hospitals</b>	
Object, % contaminated	Average Height (inches)
Rails, 34.5	34-38
Furniture, 27	18 (for chairs)
Sinks, taps and basins, 27	33-36 (for kids vs adults)
Door handles, 23.5	34-48
Flat Surfaces, 21.5	34-36 (for counters)
Hospital bed tables, 40	21.6-33.5 , 30 (for tables)
Light Switches	48

Although the aforementioned robot designs present unique solutions to the problem of decontaminating surfaces for coronavirus, they each leave room for improvement. The Blue Oceans robot excels in its user interface, its circular UV-C light design and its ease of maneuverability due to its small body. However, it falls short in its 2D mapping system which does not allow for a comprehensive map of all the surfaces in a room. The robot also requires a user to arbitrarily choose places for the robot to stop and disinfect. Because they are chosen by the user these stopping locations are often not optimized in distance or orientation to a surface and hence, often require more power to disinfect these surfaces. Lastly, this robot requires a manual safety check before use which limits the level of autonomy of which the robot is capable. On the other hand, the UVA robot excels in its use of a 3D mapping system. It also is capable of disinfecting surfaces beyond the line of sight with its robotic arm and it generates a disinfection map which allows the robot to track exactly which surfaces have been cleaned. But, this robot also has room for improvement. First, the robot has a large base that is cumbersome to maneuver in tight spaces. This means for these spaces, the robot must disinfect from a further distance which vastly reduces the robot's efficiency. This robot also follows a path selected by humans. If this path were to be optimized and computer selected, its efficiency would be increased. Lastly, the placement of the lights on the robot fit the design of the UGV that was used but more research can be done to better place these lights so that they can directly hit high touch surfaces. In all, these assets and shortcomings have led to our goal of creating a semi-autonomous robot that utilizes the arm design created by the UVA team, while maintaining the maneuverability of the Blue Ocean robot.

## Design Process

Our approach can be outlined in the following seven steps; (1) identify customer needs, (2) establish target specifications, (3) concept generation, (4) concept selection, (5) design, (6) build and (7) test, as shown in Figure 2. This structure ensures that the final product meets all customer requirements throughout its development.



Figure 2. Project approach for design and fabrication of disinfecting robot

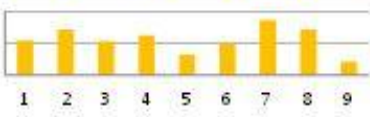

To identify customer needs, first advantages and disadvantages of current technologies were identified. Once identified, each item was translated into an interpreted need. Each need was then ranked by importance. The most critical features identified in this step are ordered and tabulated in Table 2. They were identified to relate to safety, maneuverability, effectiveness, ease of use, efficiency, and potential for autonomy.

Table 2. Customer needs results

Customer Needs Results	
Ranking	Sanitation Robot Need
1	<ul style="list-style-type: none"> <li>Has auto and manual (including remote button) shut off capabilities for motion and lights</li> <li>High rate of update in imaging tools and map update</li> </ul>
2	<ul style="list-style-type: none"> <li>Can fit through a doorway</li> <li>Is maneuverable in complex indoor environments</li> </ul>
3	<ul style="list-style-type: none"> <li>Need to quickly and efficiently disinfect a room (extendable/retractable arm with high touch point capabilities)</li> </ul>
4	<ul style="list-style-type: none"> <li>Robot is robust and easy to use (stress and corrosion analysis performed, low CG, intuitive UI)</li> </ul>
5	<ul style="list-style-type: none"> <li>Sufficient battery capability to fully disinfect a room without requiring an intermediate recharge</li> </ul>
6	<ul style="list-style-type: none"> <li>Localization and mapping capabilities possible (include SLAM sensors)</li> </ul>

Once customer needs were identified and prioritized, target specifications were established. The specifications were informed by current technology limitations and assets. The specification step allows for precision when defining what the product needs to be able to accomplish. They consist of a measurable metric, ideal, and marginal values, as pictured in Table 3. The table is formulated to calculate the relative effort that should be dedicated towards reaching each specification based on difficulty and importance.

Table 3. Target specifications

	Importance (Customer Need <sub>5</sub> )	SPECIFICATIONS:								
		Battery Life	Degree of Autonomy	Length of Smallest Profile	Time for complete disinfection	Economy of space within chassis	UV light intensity	Maneuverability	Localization / mapping	Total Mass
Direction of Improvement		↑	↑	↓	↓	↓	↑	↑	↑	↓
<b>CUSTOMER NEEDS:</b>										
Auto and manual shut off lights and/or entire system	5		3		1			3	3	
Fits through a standard doorway	5			5		4		3		
Quickly and efficiently disinfect a room	4	5	4		5		5	4	4	
Robust and easy to use (low CoG, intuitive UI)	2	2	3					4	3	
Sufficient battery capability	5	5			3	2	5			4
Maneuverable in complex spaces	4		4	5	2			5	4	
Localization/mapping capabilities	3	1	5	2	4		1	3	5	
<b>TECHNICAL IMPORTANCE, DIFFICULTY, AND PRIORITY:</b>										
Technical importance (calculated, absolute)		52	68	51	60	30	48	83	68	20
Technical importance (calculated, percentage)		10.8%	14.2%	10.6%	12.5%	6.3%	10.0%	17.3%	14.2%	4.2%
Technical importance (calculated, rank)		5	2	6	4	8	7	1	2	9
										
Units		mAh		in	min	% unused	W/m <sup>2</sup>	m/s	Y/N	kg
Marginal Target Value		10		< 30	< 120	< 30	33-50	> 1	Y	< 225
Ideal Target Value		> 15		< 3.2	< 30	< 5	45	> 2	Y	< 68
Technical Difficulty: 5 = Trivial; 1 = Very Difficult		4	1	3	3	3	5	4	1	3
Technical Priority (calculated)		208	68	153	180	90	240	332	68	60
Technical Priority (calculated, rank)		3	7	5	4	6	2	1	7	9
										

Next, concept generation provided for a transition between product specifications and a realizable product. This was broken into two parts, functional decomposition and morphological analysis. Functional decomposition allowed for the design challenge to be divided into several simpler subproblems, including drivetrain, chassis, power supply, and disinfection method. For

each subproblem, solutions were brainstormed. We then tabulated our solutions to allow for the systematic review of solution fragments and ultimately paired solutions into divergent options for concepts, pictured in Figure 4.


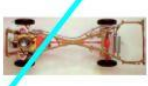



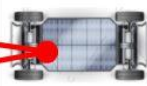
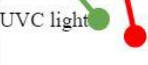
Sub functions	Solutions					
Drivetrain	4WD, 4WS	H-Drive	Mecanum	Holonomic	Drive Track	Legs
Chassis	Ladder 	X-Type 	Onset 	Offset w/ Cross member 	Perimeter 	Platform 
Power Supply	Li-Ion Battery	Hydrogen Fuel Cell	Gasoline	Capacitor	Li-Poly	NiMH - nickel-metal hydride battery
Disinfection method	UVC light 	Disinfectant sprays	Steam vapor	Ozone treatment	Antimicrobial adhesive coat	Hydrogen peroxide spray

Figure 4. Concept generation results

After concept generation, we transitioned into concept selection. For this portion of our approach, the focus was on evaluating the concepts generated during concept generation. This step was broken into concept screening and concept scoring. Concept screening allowed for an approximate evaluation to narrow the options. Concept scoring provided a careful analysis of the concepts identified in concept screening. The concept screening matrix consisted of selection criteria based on the customer needs identified in the first step (identify customer needs) and each concept was given a relative score of “better than” (+), “same as” (0), or “worse than” (-) for each criteria. Then each score awarded was totaled and modifications were considered, as depicted in Table 4. The most promising options were then analyzed using concept scoring. In this case all options considered for concept screening were continued with as each performed similarly.

Table 4. Customer screening results

Potential Solution →	Green Lines	Blue Lines	Aqua Lines	Red Lines
Selection Criteria ↓				
Battery Life	+	0	+	+
Degree of Autonomy	0	0	0	0
Time for Complete Disinfection	+	0	0	+
Economy of Space Within Chassis	0	0	0	0
Effectiveness of Disinfection	0	-	0	0
Manueverability	+	0	0	-
Quality of Localization/Mapping	0	0	0	0
Emergency Stop/Safety Functions	0	+	-	0
Sum +'s	3	1	1	2
Sum 0's	5	6	6	5
Sum -'s	0	1	1	1
Net Score	3	0	0	1
Rank	1	3	3	2
Continue?	Yes	Yes	Yes	Yes

The concept scoring matrix was developed to provide a more refined comparison. In this stage, the selection criteria were weighted by importance and each concept received a score for each criterion, as shown in Table 5.

Table 5. Customer screening results

Solution →		Green Lines		Blue Lines		Aqua Lines		Red Lines	
#	Selection Criteria ↓	Weight	Rating	Weight	Rating	Weight	Rating	Weight	Rating
1	Battery Life	5%	5	0.25	3	0.15	5	0.25	5
2	Degree of Autonomy	15%	5	0.75	5	0.75	5	0.75	5
3	Time for Complete Disinfection	5%	4	0.2	3	0.15	3	0.15	4
4	Economy of Space Within Chassis	5%	4	0.2	4	0.2	4	0.2	4
5	Effectiveness of Disinfection	20%	4	0.8	3	0.6	4	0.8	4
6	Manueverability	15%	5	0.75	4	0.6	4	0.6	3
7	Quality of Localization/Mapping	15%	5	0.75	5	0.75	5	0.75	5
8	Emergency Stop/Safety Functions	20%	4	0.8	5	1	3	0.6	4
#	Score			4.5		4.2		4.1	

Again, the concepts performed similarly with the exception of the green option. At this point the team revisited concept generation, informed by the concept selection results and produced an alternate concept that incorporated the best aspects of the winning design from step

4 (concept selection) and competitive aspects of other highly scored concepts, including a mecanum drive type and x-type frame. After this revision, the team entered the design stage. The purpose of this step was to develop a feasible product that can be built and tested that meets the specification and customer needs outlined in steps 1 and 2 (identify customer needs and establish target specifications). Included in this step is the specification of geometry, materials, and tolerances of all product parts as well as the identification of components to be purchased from suppliers. After this step, a prototype was fabricated in step 6 (build) and tested in step 7 (test). As needed, steps 5-7 were repeated until the prototype met all product specifications and customer requirements. This resulted in the design shown below in Figure 5.

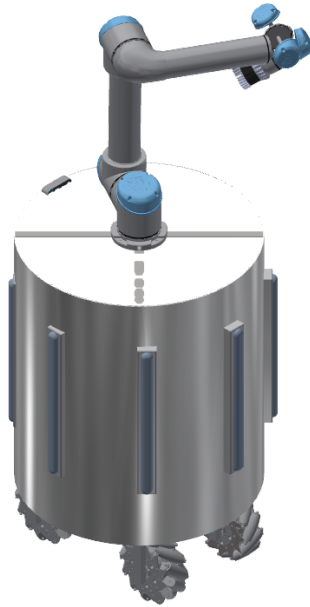


Figure 5. Initial robot design from November 2020

As the semester progressed, the team revised the project's core systems multiple times, selecting different design concepts, eventually creating the final design as described in the following section.

## **Final Design**

At this time, the team has finished working on the design of the robot by iteratively going through the design process. The robot was built using a perimeter chassis, mecanum wheels to move in many directions, lithium-polymer batteries to power the robot, and UV-C light to disinfect surfaces. These choices were made over the course of the semester in order to maximize fulfillment of the project's goals. An isometric computer-generated view of the final design of the robot is provided below in Figure 6, along with a picture of the completed robot. The team decided to name the robot Robot Operating System Infection Eliminator (ROSIE) which describes its overall functionality and primary objective.



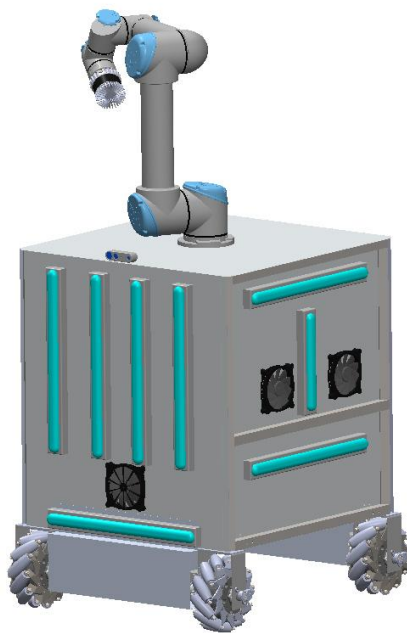


Figure 6. Left: final CAD robot design from April 2021. Right: Final assembled version of ROSIE (without light bulbs and LiDAR)

The final robot design has a square shaped chassis with side lengths of 28 inches and a height of 29 inches, not including the wheels and their associated assembly. The decision to move to a square shaped perimeter chassis design was decided to reduce manufacturing obstacles and eliminate inherent sources of uncertainty in fabrication. The height of the robot in conjunction with the Universal Robotics UR-5 robotic arm enables the robot to disinfect surfaces up to 48 inches off the ground and higher, such as light switches and doorknobs. The decision to utilize the smaller UR-5 arm over the larger UR-10 arm was made to maintain the robot's desired reach for disinfection, while reducing tipping and stability concerns. The maximum payload allowed for the UR-10 arm (22 lb) is much greater than the UR-5 (11 lb) and this greater strength would not be utilized for this application. The perimeter-type chassis was more than sufficient to support the robotic arm atop the frame and heavy internal components required. An intermediate shelf was included in the center to allow for more surface area for mounting components in order to maintain a smaller profile.

The wheels selected are 8-inch Mark Koors mecanum wheels from AndyMark. These were chosen for their degree of mobility, simplicity of programming, reduced mounting complexity, reduced number of motors required, size, availability, cost, and load capacity. The motor selection was governed by power requirements and target operating conditions. A computer generated image of one of the drivetrain assemblies is shown below in Figure 7. The robot was predicted to weigh about 250 lbs with the target speed and acceleration defined as 1 m/s and 2 m/s<sup>2</sup> respectively. Using these parameters, target wheel operational speed and torque

for each motor was calculated to be 142 RPM and 17.4 Nm, respectively. This estimate was made assuming rotational inertia of the wheel, rolling resistance, air drag, incline, and internal friction from the bearings are negligible and accommodates for the wheel type. The AndyMark 2.5-inch CIM Motor was found to be capable of operating at this target point using a 100:1 CIM Sport gearbox and fits within relevant geometric constraints. Additionally, the operating point was checked to ensure that wheel slip will not occur. Detailed calculations can be found in Appendix A.i. Testing of the completed robot's speed yielded speeds in excess of 0.6 m/s. While this speed was short of the target established in design, it was deemed acceptable for the purposes of disinfecting indoor spaces as high speeds and accelerations would not be used. Furthermore, two skid plates, manufactured by Protocase, surrounding the front and rear motor assemblies provide protection from dirt, dust, and possible collisions.

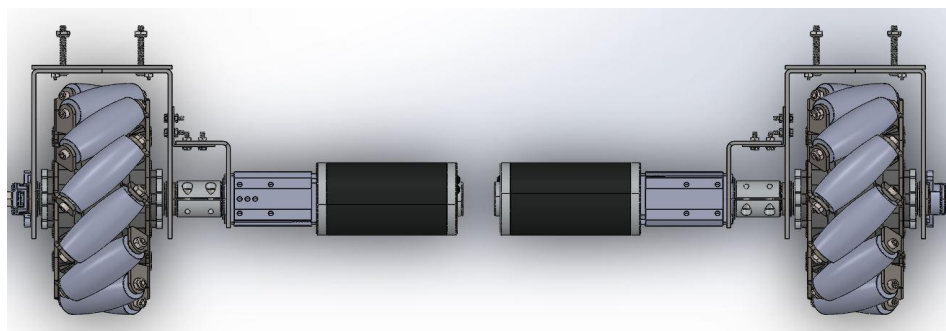


Figure 7. Final motor assembly design from February 2021. From left to right: encoder, wheel assembly, hex shaft coupler, gearbox, brushed DC motor

A tipping analysis was conducted using moment calculations as shown in Appendix B. These calculations used an overestimate of the robot's weight including the arm and a potential worst-case scenario tipping condition. The analysis indicated that despite the robot's height, the weight of the frame, arm, and heavier components such as batteries and computer components prevent tipping conditions from occurring in standard use. A force of nearly 25 lb at a specific location, at a specific angle, while the robotic arm is in particular orientation would be required to influence the stability of the robot. All other external forces would need to be higher than 25 lb in order to tip the robot. It was deemed that this was sufficient since such a force could not be accidental.

To provide adequate disinfection, 14 UV-C tube lamps were mounted on the robot's body to provide disinfection of surfaces and the surrounding air. Five 19.5-inch tube lights were placed on the front with one on the skid plate, three were placed on each side in an 'I' formation (two 19.5-inch and one 9-inch each), two were placed on the back side (a 9-inch and a 12-inch), and one 19.5-inch was placed on the arm. The initial light design went through several iterations of redesign before this configuration was selected. The primary change to the light design was that the lights on both sides of the robot were recessed and mounted internally in order to save about 4 inches of room on the robot's profile, allowing for increased maneuverability through doorways. Because of this, an 'I' formation was found to be the most advantageous configuration for the lights that had been ordered, given the limitation of the middle shelf which obstructed the ability to place the larger 19.5-in lights vertically.



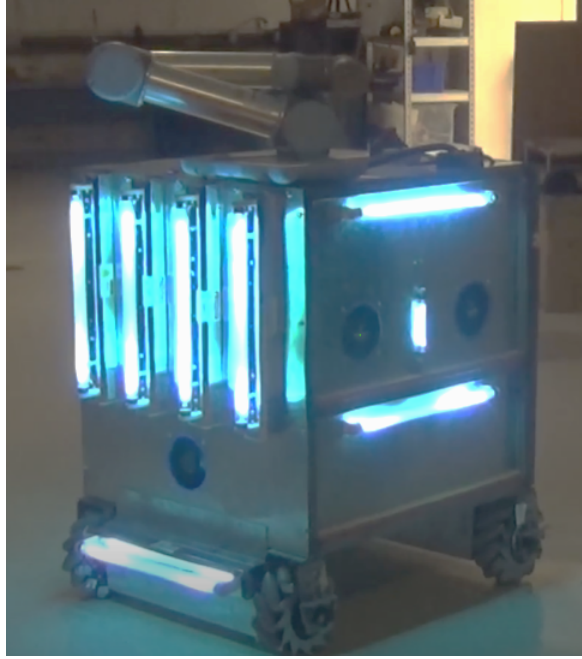


Figure 8. Robot light design front and left side panel

The front and arm of the robot is where the robot's primary disinfection takes place. Because of this, the arm was given the largest disinfection lamp for maximum power output. To calculate power output the following two formulas were used;  $E_{k^{19.5in}} = \frac{I_{k^{vertical}}(\theta_k)}{L_{k^{\wedge}}^{1.06}}$ , where

$I_{vert}(\theta_k) = 89.75 \times 10^{-6} W/cm^2$  and  $E_{k^{12in}} = \frac{I_{k^{spot}}(\theta_k)}{L_{k^{\wedge}}^{1.27}}$ , where  
 $I_{vert}(\theta_k) = 16.73 \times 10^{-6} W/cm^2$ . These calculate power output for the 19.5-in and 12-in lights respectively where  $I(\theta_k)$  is luminous intensity,  $L_{k^{\wedge}}$  is distance of light projection onto surface,  $x_k$  is point of light source orientation at time step k,  $E_k$  is UV-C light power at time K, and  $\theta_k$  is angle of light orientation.

Using this equation, the front panel has the most power output with a theorized  $2.72\mu W$  of power per  $cm^2$  from a distance of 1 meter away while the sides each output  $1.44\mu W$  as calculated in Appendix C and E. This was determined to be sufficient as it is predicted to take the robot less than 43 minutes to disinfect an average hospital room with the front side alone as shown in Appendix D (Cahnman 2017). The fifth light on the front that is located on the skid plate disinfects the floor of any aerosols that could contain the virus falling in the air. The choice to place lights on the back side of the robot despite the long distances the light will have to travel and its inverse squared relationship with power was validated in Appendix C, with a power generated of  $0.15\mu W$ .

A UV-C spot lamp and Ouster OS-1 LiDAR mounted on the end of the UR-5 robotic arm provide mapping capabilities as the robot maneuvers around the room and also provide precise spot disinfection at set distances from objects. The OS-1 LiDAR provides much needed accuracy

in distance measurement, as the robotic arms spot lamp must maintain a consistent distance from various surfaces for effective disinfection. The development of a point-cloud map of the room the robot occupies is also necessary for further autonomous development. Further sensing capabilities were provided by a fisheye web camera. This camera, mounted on the front side of the robot facing outwards, helps the operator to maneuver the robot around environments to optimal locations for disinfection. The robot's computer system provides visualization and control of sensor imaging, and allows for Secure Shell Connection (SSH) via Wi-Fi for remote control. An Arduino connected to the computer via USB sends Pulse Width Modulation (PWM) signals to the motor controllers via jumper cables. A Logitech gaming controller connected via Bluetooth to the computer is used to send commands to the motor controllers, as well as turn on and off the lights.

All of the above features of the robot were mounted either onto the carbon steel frame of the robot, wooden shelving, or onto the aluminum 6061 sheet metal 0.025" thick attached to the frame. Aluminum 6061 was chosen for its tensile strength and ease of machining as multiple sections of each sheet were required to have holes cut out of them for mounting of the fans and lights. An engineering drawing of the frame can be seen in Appendix E. The frame was made of one-inch carbon steel square tube. The material for the frame was chosen to be carbon steel because of the general purpose performance of the alloy, the high strength-to-weight ratio, and for good machining properties. The frame consists of four vertical bars placed at the corners of the square shape. The top, middle, and bottom of the frame consist of crossed bars that support the inner components, and provide a mounting location for the shelf and other components.

An important electrical component is the lithium-polymer battery as it is the source of power for the other electrical devices. Based on the system that this project is inspired from, 25.9 volt batteries were recommended. The summation of the maximum power consumption of each electronic component was calculated to determine the best wire gauge. Though using the maximum power was an overestimation and all electrical components using their maximum power consumption simultaneously was not likely, it was a safety and precautionary measure taken to prevent possible and unforeseen mishaps like blowing devices that can compromise the functionality and safety of the robot. Using the Ohm's Law equation,  $P = VI$ , ( $P$  is power in watts,  $V$  is voltage in volts, and  $I$  is current in amps), the total maximum power consumption for the robot is theoretically 2,049.97 W. The voltage and current of each direct current (DC) powered component and the power consumption of the alternating current (AC) powered devices were given to calculate that number. Furthermore using the same equation, the current needed to power the entire robotic system is approximately 79.15 amps. A 10 gauge wire is needed from the power source to run the rest of the system. Also, sub-power sources within the system include a DC-DC step down converter and DC-AC converter. The total maximum power consumption of the devices connected to the DC-DC step down converter and DC-AC converter are 971.97 W and 1,078 W, respectively. The current needed for the DC-DC step down converter is 37.82 amps and for the DC-AC converter is 41.62 amps. A 10 gauge wire is theoretically needed for both devices. In terms of the robot's run-time, another battery is needed for an operation of at least 30 minutes at maximum power. The robot includes a second lithium-polymer battery. The two batteries are connected in parallel, which doubles the amount of amp-hours and increases the run-time that can be provided to the system. Detailed calculations of power and current are provided in Appendix F. The chart that gives corresponding wire gauge to current is provided in Appendix G.

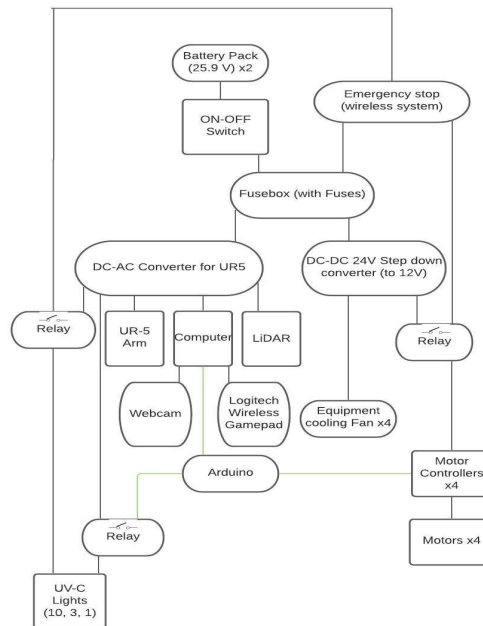


Figure 9: Electrical Schematic of the Robot

As mentioned before, major electrical components in the interior of the robot include two lithium-polymer batteries that are rated for 25.9 volts DC each. Next, the parallel-connected batteries are wired to a fuse box. The power from the fuse box will be distributed to different electrical components that are connected to it. Additional electrical components include a DC-DC step down converter, a DC-AC converter, and a wireless emergency stop system. The DC-DC step down converter decreases the 25.9 voltage from the battery to 12 volts which is used to power four 12-volt motor controllers for the driving system and 12-volt fans to cool the interior of the robot. The DC-AC converter gets its power from the DC power supply from the fuse box, yet transforms the DC power to AC power. AC power is required for the computer, lights, and UR-5 robot arm, which are all connected to surge protectors connected to the DC-AC converter. Lastly, the wireless emergency stop receiver receives a 25.9 volt supply directly from the battery. The emergency stop button transmitter controls the power to the receiver. A detailed depiction of the connections is in Figure 9 above.

The inclusion of relays (between DC-DC converter and motor controllers, as well as the DC-AC converter) controlled by a wireless emergency stop button allows the robot to be stopped whenever necessary. The receiver, while connected to the battery, continuously provides power to the coil of the relay until the emergency stop button (wireless transmitter) is pushed and signals the halting of power to the coil. This causes an open circuit that stops power from going to the motors. The same principle applies to the relay connected to the lights (which is also connected to the wireless emergency stop). Another relay between the lights and the DC-AC converter controlled by Arduino pins allows the lights to be shut off independently of the motors, via button press of the Logitech controller. The relays used in the robot are designed as normally open when no current is going to the coils.

The components of the frame were cut out of carbon steel using a perpendicular saw machine at Lacy Hall, and then welded together by a local welder. Once all internal components were assembled, mounted, and tested, external components were mounted to the aluminum sheets and attached to the frame. The rear aluminum sheet of the robot was mounted using hinges and a sliding bolt allowing for access to internal components of the robot (such as the batteries for easy recharging). The back panel door was reinforced with spare metal from the frame in order to keep it rigid. Images showing the access panel and its function are shown below in Figure 10.

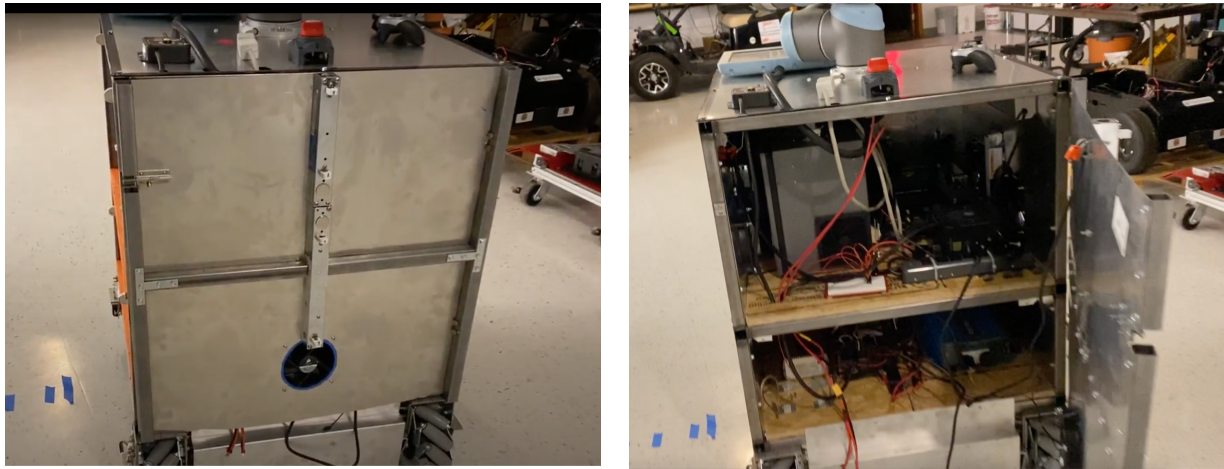


Figure 10: Left: ROSIE access panel closed, Right: ROSIE access panel open

## **Validation**

### **Stress Test**

A stress test was simulated on the frame using drafting software. This was to ensure that the frame would support the weight of all components contained within. A 100-pound weight was placed upon each shelf. This weight was chosen because it was far beyond any weight that was expected. As a result of the simulation, the maximum deflection of any part of the frame was 0.015 inches and the maximum stress was 10 ksi. The stress result is less than one third of the yield stress of the carbon steel used (32 ksi). This ensured that there would be no structural failure of the frame.

### **Torque Test**

Motor output was tested using a torque test. This was to confirm how close to rated specifications the motor achieved. This test was performed by suspending the robot so that the drivetrain was 1.5 meters away from the ground. Then, a bucket was hung from the hubs attached to either side of a single wheel using wire. The bucket was suspended to the hubs instead of the wheels because the geometry of mecanum wheels would cause the wire to roll off as the wheel rotated. Using the hubs, a level surface was achieved and since they were bolted to the wheel, the difference with respect to the test mechanics was negligible. Heavy bars of metal were then incrementally added to the bucket until the load the robot would be subject to in

application was well exceeded. The final weight of the bucket was 19.25 kg. At this load, there was no appreciable reduction in output of the motor. The test was stopped at this point because the wire suspending the bucket broke and expected operation torque had been well exceeded as had the stall torque reported by AndyMark. The moment arm of the setup was 0.03 meters, which is the radius of the hubs. The force applied was equal to the mass of the loaded bucket (19.25 kg) multiplied by the acceleration of gravity ( $9.81\text{m/s}^2$ ), which is 188.8 N. The torque applied then can be calculated as the product of the force and moment arm, 188.8 N and 0.03 m, respectively. Thus, the torque at which the test was stopped and no deceleration of the wheel was observed was 5.67 Nm. The rated stall torque of the motor (2.42 Nm) is far less (difference of 3.25 Nm) than the torque we were able to achieve with the setup connected to two 25.9V lithium-polymer batteries. The motor performed better than expected. In service, each motor will encounter far less torque than was tested during this experiment due to the high gearbox ratio of 100:1 resulting in a torque on each wheel of about 0.11 Nm as calculated in Appendix A.ii.

### Lights Test

To validate the light design, tests were conducted using a UV Light meter held at known distances away from each side at a height of about 24 inches. Measurements for the front and side panels were taken at increments of 0.1 meter from 0.1 meter to 1 meter away. Measurements for the back panel were taken at distances 2.07 meter to 4.15 meter at increments of about 0.3 meter. Each distance range was selected to represent the range that is expected to be disinfected by each of the given sides in a typical hospital room. The front and side panel are expected to operate very close to surfaces while the back panel was given a range between the closest object it will likely disinfect, a hospital bed, and the longest distance it could be from the far end of an average hospital room while still being wheelchair compliant (see Appendix C for hospital room dimensions). These measurements were compared to theoretical calculations of power in the same range and are displayed in Figure 9 below.

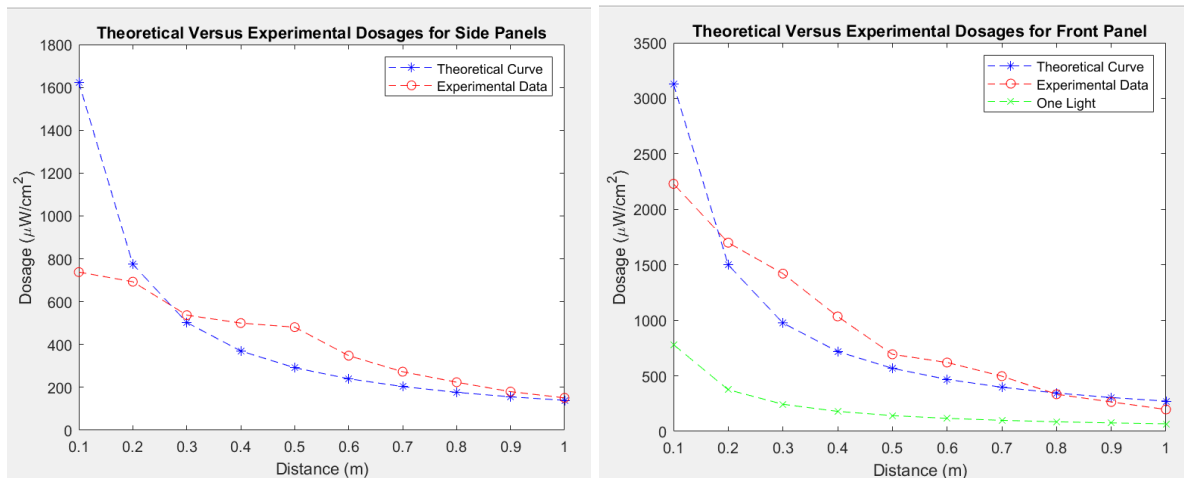


Figure 11. Theoretical versus experimental dosages for side and front panels

The experimental curves for both the side and front panels show a higher dosage being delivered at almost all of the distances compared to the theoretical curve. This was expected as the theoretical calculations treat the lights as point sources rather than a tube. The increased dosage is also a product of the design choice to use a silver, reflective body for the robot in order

to maximize output dosage reaching nearby surfaces. Both of these tests show a dip in the dosage curve around 0.1 to 0.2 meters. This is because as the UV meter was brought closer to the robot, it was placed directly in front of one light while light from the surrounding lights was no longer able to reach it. As angle of incidence is very important in determining power output, it is to be expected that as the light from some of these tubes are no longer able to reach the monitor, the dosage will fall below the theoretical calculation for all the tubes compounded. The graph of the front panel is also compared to the theoretical dosage from one light to provide a baseline and show the effectiveness of choosing to use more than one light for the robot. From these results, each panel exceeds the minimum output power and time for disinfection that were proposed in the design.

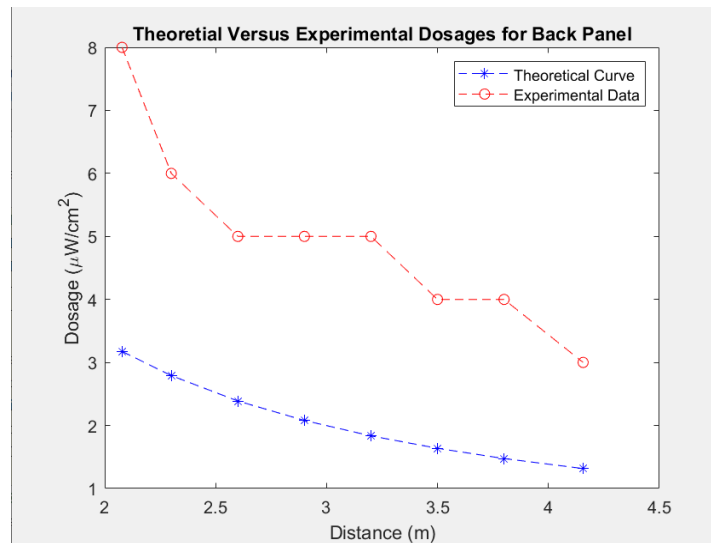


Figure 12. Theoretical versus experimental Dosages for back panel

The experimental curve for dosage as seen above is well above the theoretical curve. In the range for 2 to 4.5 meters, there is no dip in the curve present as the UV light meter never entered a range that one of the lights could not meet. This shows that the design delivers almost three times more power than the predicted amount in this range.

## Operations Manual

In order to initially operate ROSIE the following must happen:

1. Both batteries are charged to the same capacity and plugged into their respective cables.
2. A monitor, keyboard, and mouse must be plugged into the computer. Make sure the computer has the Linux operating system and the Robot Operating System (ROS) installed.
3. All light bulbs must be connected to their respective housing on the outside shell of the robot.

After all of these steps are completed, you may turn the power switch on the upper inner tier of the robot, rotating the large red switch from red to green. This will provide power from the batteries to every element of the robot. When this happens, the UV-C lights will not turn on because the relay that they are connected to has not allowed for power to turn the lights on yet.

We will get to how you will be able to turn these on down below. Once the switch has been turned, make sure to turn on the computer via its power button which will highlight in blue after depressed. If you forget to do this, you will not be able to operate ROSIE.

Now that power is supplied to the robot and the computer is on, you may be asked to input the username and password for the computer. The username is ROSIE and the password is password. From the computer, there are a few things you can do before you can unplug the monitor, keyboard, and mouse:

1. Activate the drivetrain and toggling of the UV-C lights
2. Start the USB camera
3. Start the LiDAR

In order to start up the commands for each of the three processes above, you have to launch separate terminal windows. When we specify to launch a terminal window, do the following on the keyboard: Ctrl + Alt + T.

To operate the robot, the user must use a wired or wireless controller. We recommend using a wireless controller so you are not limited by the length of a cable in order to operate ROSIE. To start up the commands for the drivetrain do the following:

1. Open a new terminal window
  - a. Type “roscore” and press enter
2. Open a new terminal window
  - a. Type “roslaunch joy joy\_node dev:=/dev/input/js0” and press enter
3. Open a new terminal window
  - a. Type “cd Desktop” and press enter
  - b. Type “roslaunch load joystick\_param.yaml” and press enter
  - c. Type “roslaunch joy\_teleop joy\_teleop.py” and press enter
4. Open a new terminal window
  - a. Type “roslaunch rosserial\_python serial\_node.py /dev/ttyACM0” and the press enter

The user should now be able to have full control of the robot via a wired or wireless controller. The figure below shows the control scheme that allows the robot to be moved around. ROSIE can be finicky so if you ever find that ROSIE does not do what you want her to do, let go of left back (LB), then press and hold LB again and any issues should fix themselves.





Figure 13. Control scheme for ROSIE

Next, we will discuss how to activate the USB cam that ROSIE is equipped with. Do the following steps to get the USB cam working:

1. If roscore is already running skip this step but if not, open a terminal window
  - a. Type “roscore” and press enter
2. Open a new terminal window
  - a. Type “cd myworkspace” and press enter
  - b. Type “roslaunch usbcam.launch” and press enter

If you get an error after part 2b, make sure that you check that the USB cam is actually plugged in. Otherwise, you should see an image for the USB cam on the desktop.

Lastly, we will talk about starting up the LiDAR. It is a bit finicky, so we cannot get it to publish topics at this point, but we can verify that it works. Do the following steps in order to get it working:

1. If roscore is already running skip this step but if not, open a terminal window
  - a. Type “roscore” and press enter
2. Open a new terminal window
  - a. Type “cd myworkspace” and press enter
  - b. Type “source devel/setup.bash” and press enter
  - c. Type “roslaunch ouster\_ros ouster.launch  
sensor\_hostname:=os1-992004000789.local \  
udp\_dest:=169.254.167.219 \  
lidar\_mode:=1024x10 viz:=true

The figure below should be what comes up once step 2c is executed correctly.



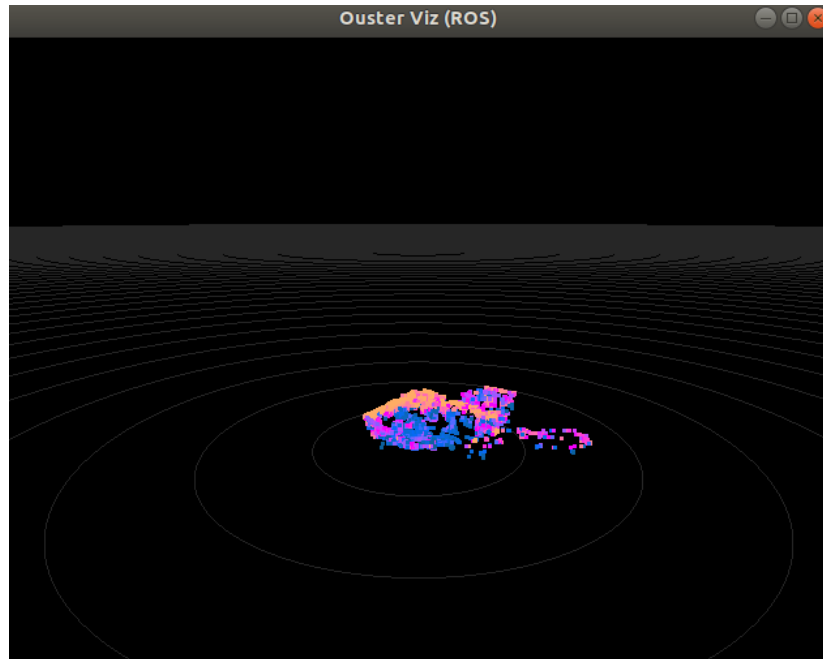


Figure 14. Verifying that LiDAR works

An error that could arise with this is that the `udp_dest` may have been changed so you may need to open a new terminal window, type `“ip addr”`, and compare the `inet` to what is currently written in `udp_dest`.

Additionally, if you do not want to plug in a monitor, keyboard, and mouse to ROSIE you can access all of the things described above using a method called Secure Shell Protocol (SSH). Below are the steps you can take in order to ssh and control ROSIE remotely:

1. Boot up a laptop running Ubuntu 18.04 with all relevant ROS software packages installed, and connect it to the VICTOR2 router.
2. By default ROSIE will be connected to VICTOR2- if this is not the case, she will need to be connected to the router for Secure Shell Protocol (SSH) control with keyboard and mouse.
3. In a terminal window, connect to ROSIE using the command `“ssh user@192.168.1.129”` and when prompted, enter the password: `“password”`.
4. Start `roscore` in that terminal window.
5. For each topic/launch file used, a new terminal window connected to ROSIE is required. The commands required are the same as explained above.

The following is what the user can do right now to improve the system of ROSIE:

1. Integrate the usb cam and LiDAR together in RTAB map and get the topic `find_object_2D` working
2. Load up Dean’s mapping code onto ROSIE and integrate it with the usb cam and LiDAR
3. Add variable speed to the robot drivetrain code (it is located on the desktop and it is called `“fourmotorcontrolwithcontroller”`)

## Conclusions and Future Work

The main goal for the team's senior design project was to create an autonomous robot that can disinfect a room semi-autonomously. Objectives during the Fall 2020 semester were to create a design for a robot that has better mobility relative to previous designs, safe for humans in or near its environment, and to determine an effective and efficient disinfection method. The team closely analyzed past efforts and other sanitation robotic systems and determined the best ways to improve upon existing systems for the project. After doing meticulous research and defining customer needs and target specification, the team determined that the robot's highest priority is safety. The second priorities were mobility and effectiveness. By developing a Concept Generation map, the best combination of chassis, drivetrain, power supply, and disinfection was determined. A system with a perimeter chassis, mecanum drive train, Lithium ion power supply, and UV-C light disinfection was found to be the optimal combination for the system. The team has created a design that accounted for the top priorities. The design of the robot at the end of the Fall 2020 semester was narrow enough to fit conventional doorways and tall enough to reach high touch points on surfaces. The addition of a UR-5 robotic arm was used to help with sanitation. The arm is necessary to increase the flexibility in disinfecting difficult places beyond the line of sight of the robot. UV-C lights are a simple method of sanitation, and the number of lights necessary and the positions of each light on the robot to maximize sanitation as much as possible were examined.

In the spring, designs for all subsystems evolved to reflect new considerations by the team. Parts were ordered, the bill of materials was completed, and assembly began. The team faced a number of barriers including university closures and delays to parts orders (including several parts that did not arrive by the completion of the project). Additionally, unforeseen electrical setbacks occurred after complete assembly. Though this feature has functioned fully, the UV-C lights would not toggle on and off while pressing its designated button on the Logitech controller during the final demonstration. This could have been an electrical wiring issue, a faulty relay, or a software issue. In manufacturing the drivetrain mounting system, it was determined that future custom systems should be in as few parts as possible to reduce tolerance stackup that inhibited the assembly process. There were also many unanticipated points at which systems needed to be deconstructed and built again as the next stage of complexity was added. There were substantial modifications to the design after parts arrived, including adapting to recessed lights and a hinging access panel. Ultimately, the team found that the electrical system was the major source for issues and troubleshooting the causes was tedious, challenging, and did not always end in resolution. Additionally, despite it being several inches smaller than the previous design, the robot is still large relative to the space it must navigate within. While the size does not keep it from entering a typical doorway, it takes time and skill to accomplish this task. For this reason, the team is proposing a new design for future work in disinfection in complex indoor spaces that takes into consideration what was learned throughout this project.

The new robot design is 18 by 21 inches achieving a reduction in footprint of 55%. This is achieved mainly by switching to a sprocket based drivetrain (detailed in Appendix A.iii) similar to that shown below in Figure 15, which would reduce the total width of the robot to 20.5 inches.

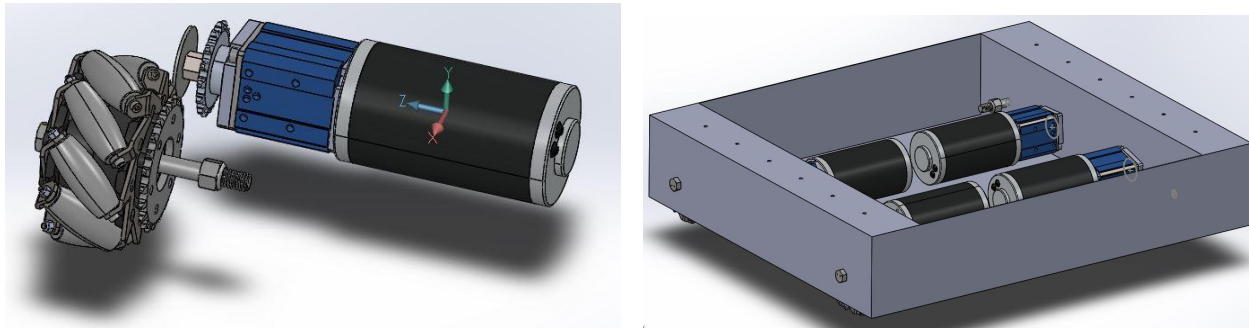


Figure 15. Initial proposal for sprocket based drivetrain.

Since the profile of the robot would be smaller, increasing the height and adding one more tier as shown below in Figure 16 would create the space needed for all internal components. The proposed robot uses the mecanum wheel type and a single custom mounting piece that performs the job of supporting the structure on the drive train and protecting the drivetrain from the environment. The smaller profile would eliminate the need to post the bodies of side lights inside the robot and a smaller and lighter robotic arm may help reduce the internal space required.

While all systems are functional at a fundamental level on the current robot, future software work will include; further developing mapping capabilities and navigation with visualization software such as RViz or RTAB map, integrating autonomy into the control of the UR-5 robotic arm, and autonomous object detection using a ROS package find\_object\_2d while using the fisheye camera.

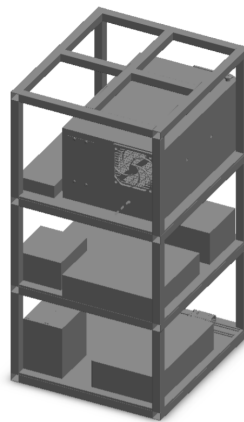


Figure 16. Proposal for chassis with 55% reduced footprint, with some internal components included

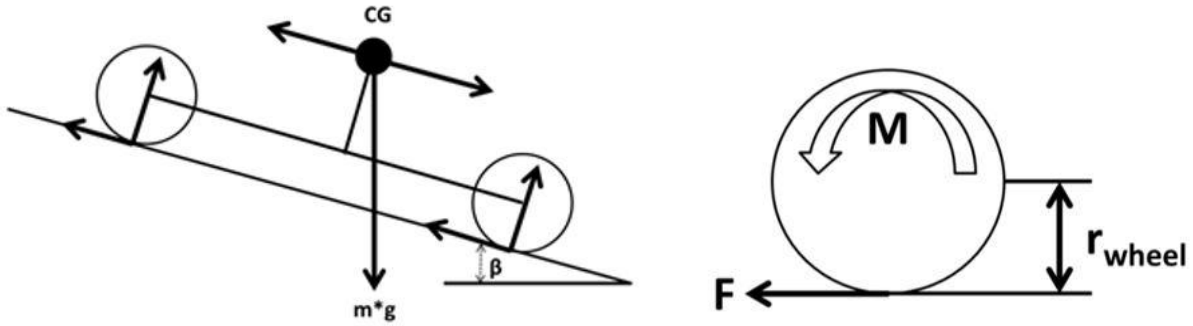
## References

- Aston, W. J. (1992). Product design and development. In Biosensors and Bioelectronics (Vol. 7). [https://doi.org/10.1016/0956-5663\(92\)90013-D](https://doi.org/10.1016/0956-5663(92)90013-D)
- Blancou J. (1995). History of disinfection from early times until the end of the 18th century. *Revue scientifique et technique* (International Office of Epizootics), 14(1), 21–39.
- Cahnman, Sheila. (2017, May 3). Design units for short-stay patient units. Retrieved May 8, 2021, from <https://www.hfmmagazine.com/articles/2841-design-guidelines-for-short-stay-patient-units#:~:text=A%20typical%20patient%20room%20size,each%20side%20of%20a%20bed.>
- Conte, D., Leamy, S., Tomonari, F. Design and Map-based Teleoperation of a robot for Disinfection of COVID-19 in Complex Indoor Environments. ( n.d.) Retrieved December 1, 2020, from <https://mail.google.com/mail/u/0/#label/CAPSTONE/FMfcgxwJXxtFwdmGrlbHQwGGscrNPRXv?projector=1&messagePartId=0.1>
- Cresswell, K., & Sheikh, A. (2020). Can disinfection robots reduce the risk of transmission of SARS-CoV-2 in healthcare and educational settings? *Journal of Medical Internet Research*, 22, 9–11. <https://doi.org/10.2196/20896>
- Edwards, E. (2020). Amid confusion, WHO clarifies that COVID-19 can be spread without symptoms. Retrieved September 24, 2020, from NBC News website: <https://www.nbcnews.com/health/health-news/amid-confusion-who-clarifies-covid-19-canbe-spread-without-n1228426>
- How coronavirus spreads. (2020). Retrieved September 24, 2020, from <https://www.cdc.gov/coronavirus/2019-ncov/prevent-getting-sick/how-covid-spreads.html>
- Hu, D., Zhong, H., Li, S., Tan, J., & He, Q. (2020). Segmenting areas of potential contamination for adaptive robotic disinfection in built environments. *Building and Environment*, 184(June). <https://doi.org/10.1016/j.buildenv.2020.107226>
- Intelligent Sterilization Robot. (n.d.). Retrieved May 8, 2021, from Time Medical Systems website: <https://www.time-medical.com/intelligent-sterilization-robot>
- Keutel, S. (2020, August 6). 9 disinfection robots fighting the coronavirus tectales tagging medical technology. Retrieved May 8, 2021, from TecTales website: <https://tectales.com/bionics-robotics/9-disinfection-robots-fighting-the-coronavirus.html>
- Mitchell, E. The Most Contaminated and Most Touched Surfaces in a Patient Room. (2020, May 27). Retrieved December 1, 2020, from <http://blog.eoscu.com/blog/the-most-touched-and-most-contaminated-surfaces-in-a-patient-room>

- Mohammed, M. N., Aziz, E. abd, Arif, I. S., Al-Zubaidi, S., Bahrain, S. H. K., A.K., S., & Eddy, Y. (2020). Design and Development of Spray Disinfection System to Combat Coronavirus (Covid-19) Using IoT Based Robotics Technology. *Revista Argentina de Clínica Psicológica*, 29(5), 228. <https://doi.org/10.24205/03276716.2020.1024>
- Mortensen, J. (2020, June 18). Six Months of Coronavirus: Here's Some of What We've Learned. The New York Times. Retrieved from <https://www.nytimes.com/article/coronavirus-facts-history.html?searchResultPosition=9>
- Schaffzin, J.K., Wilhite, A.W., Li, Z., Finney, D., Ankrum, A.L., Moore, R. (2020). Maximizing efficiency in a high occupancy setting to utilize ultraviolet disinfection for isolation rooms. *American Journal of Infection Control*, 48, 903-909.
- Talbot, V. (2019, October 1). What gauge wire Do I need FOR Amp? Explained! Retrieved May 12, 2021, from <https://99carstereo.com/what-gauge-wire-for-amp/>
- Ulrich, K. T., & Eppinger, S. (1999). Product Design and Development (2nd ed.). New York: McGraw-Hill/Irwin.
- UVD Robots. (n.d.). Retrieved Dec 2, 2021, from Green Instruments website: <https://greeninstruments.com/products/uv-disinfection/uvd-robots/>
- Walsh, B. (2020, March 25). Covid-19: The history of pandemics. Retrieved May 8, 2021, from BBC Future website: <https://www.bbc.com/future/article/20200325-covid-19-the-history-of-pandemics>
- What to do if you were potentially exposed to coronavirus disease (COVID-19)? (2021, May 4). Retrieved May 8, 2021, from Virginia Department of Health website: <https://www.vdh.virginia.gov/coronavirus/local-exposure/>
- World Health Organization. Coronavirus disease (COVID-19). (2020, December 02). Retrieved December 02, 2020, from <https://www.who.int/emergencies/diseases/novel-coronavirus-2019>

## Appendix A

### i) Calculation of target operating points



$$v_{strafing} = \frac{v_{max}}{0.66} = \frac{1 \frac{m}{s}}{0.66} = 1.52 \frac{m}{s}$$

$$a_{strafing} = \frac{a_{max}}{0.66} = \frac{2 \frac{m}{s^2}}{0.66} = 3.03 \frac{m}{s^2}$$

$$n_{wheel}(RPM) = \frac{1.52 \frac{m}{s}}{2\pi(0.1016 m)} * \frac{60 sec}{1 min} = 142.4 RPM$$

$$F = 226.7 kg * 3.03 m/s^2 = 687 N$$

$$M = \frac{687 N}{4 wheels} * 0.1016 m = 17.4 Nm$$

$$M_{trac} = \frac{226.7 kg}{4 wheels} * 9.81 m/s^2 * 0.5 * 0.1016 m = 28.2 Nm$$

### ii) Calculation of expected operating point for current robot

Acceleration = 2 m/s, Velocity = 0.5 m/s, Wheel radius = 0.1m, Mecanum wheel factor,  $q = 0.66$

Mass = 116.19 kg, Gearbox ratio,  $i = 100$ , Gearbox efficiency,  $e = 0.8$

$$n_{desired} = \frac{v*60*i}{q*2*\pi*r} = \frac{0.5*60*100}{0.66*2*\pi*0.1} = 7120 RPM$$

$$F = \frac{ma}{0.66} = 116.19 * 9.81/0.66 = 352.1 N$$

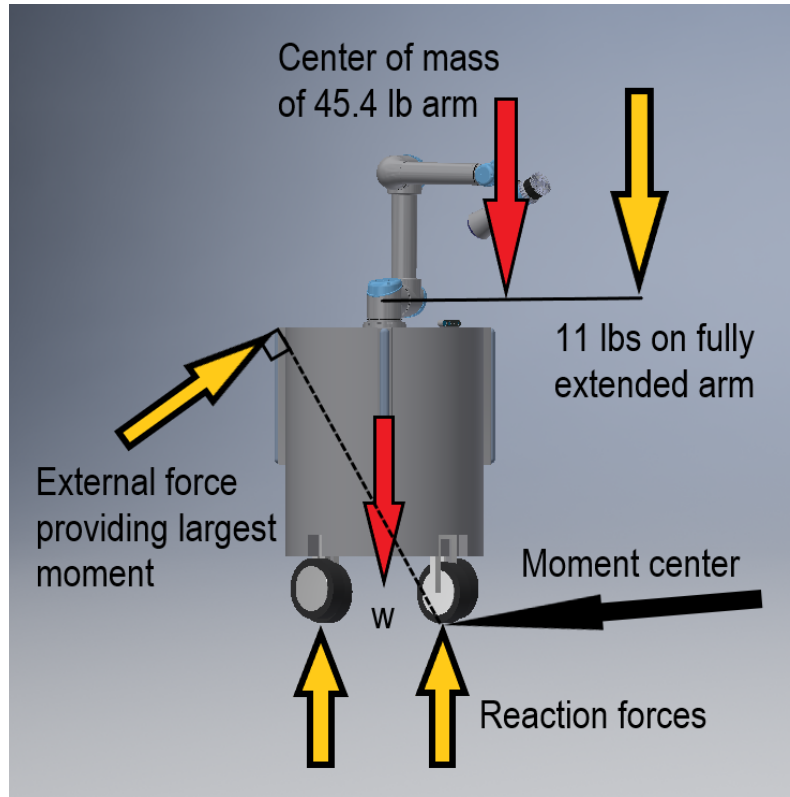
$$Torque, M = \frac{F*r}{number of wheels*i*e} = \frac{352.1*0.1}{4*0.8*100} = 0.111 Nm$$

$$\text{Power, } P = \frac{M \cdot n \cdot 2}{60 \cdot \pi} = \frac{0.111 \cdot 7120 \cdot 2}{60 \cdot \pi} = 83.35W$$

iii) Bill of materials for proposed drivetrain

Description	Part Number	Name
Motor	am-0255_16T	2.5 in. CIM Motor with 16 T Pinion
Gearbox	am-4008_020	CIM Sport Gearbox HD 20:1
Gearbox Spacer	am-3787	57 & CIM Sport Gearbox Face Mount Spacer - 0.25" thick fyi
Drive Sprocket	am-2375	35 Series 15 Tooth 500 Hex Aluminum Sprocket
Washer for Gearbox	am-1523	#10 Fender Washer
Retaining screw for gearbox	am-1541	10-32 x 0.375 in. Black Oxide BHCS with Nylon Patch
Wheels	am-3067	4 in. HD Mecanum Wheels - Bearing Bore, Full Set
Bearings	am-4464	3/8 in. Round ID Shielded Bearing (1614ZZ)
Sprocket	am-0216	35 Series 22 Tooth Round Aluminum Sprocket
Mount Sprocket to Wheels	am-1266	10-24 x 1.25 in. Thread Forming Screw Hex Washer Head
Axal	91247A639	Medium-Strength Grade 5 Steel Hex Head Screw Zinc-Plated, 3/8"-16 Thread Size, 3-3/4" Long
Nut for Axal	am-1054	3/8-16 Nylock Nut
Spacers	am-3948-063	1/2 in Hex Molded Spacers - 0.063

## Appendix B



For the robot to first be stable, the sum of moments about the moment center is zero:

$$\Sigma M = 0$$

The reaction forces both have no moment. One goes through the moment center and the other is zero when the robot begins to tip.

Moment for the weight of the robot is  $7.78 * w$  where 'w' is to be determined.

Moment for the weight of the arm is  $-179.10$

Moment for an eleven pound payload at the end of the arm is  $-282.94$

Moment for an arbitrary push is  $-43.97 * P$  where 'P' will be the maximum push.

The Sum of moments is:

$$\Sigma M = 7.78 * w - 179.10 - 282.15 - 43.97 * P$$

Solving for 'P' as a function of 'w':

$$P = \frac{7.78 * w - 462.13}{43.97}$$

'w' is currently unknown but with an estimate of  $200lb$ . then 'P' must be greater than  $24.87lb$ ., a push that is much more than accidental.



## Appendix C

### Light Calculations for Rectangular Body

#### Assumptions:

- Robot 1m away <sup>(100cm)</sup> - Robot dimensions 26" by 26" (71.12cm)
- need 10/20 mJ/cm<sup>2</sup> to be clean

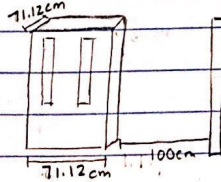
#### Equation:

$$E_k^{vert} = \frac{I^{vert}(\theta)}{L_k^{1.06}} = \frac{89.75 \times 10^{-6} \text{ W/cm}^2}{L_k^{1.06}}$$

#### Max # lights on a face:

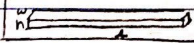
$$66.04 / 6.6675 = 10.67 \text{ 10 lights}$$

↑ light width



#### Light Dimensions:

- length: 19.5" or
- width: 2.625" or 6.6675
- height: 3.5"



One light on Front:  $E_k^{vert} = \frac{89.75 \times 10^{-6} \text{ W/cm}^2}{(100)^{1.06}} = 6.8 \times 10^{-7} \text{ W}$

Two lights on Front:  $E_k^{vert} = 2 \left( \frac{89.75 \times 10^{-6} \text{ W/cm}^2}{(100)^{1.06}} \right) = 13.6 \times 10^{-7} \text{ W}$

Three lights:  $20.4 \times 10^{-7} \text{ W}$

Four lights:  $27.2 \times 10^{-7} \text{ W}$

★ increases by  $6.8 \times 10^{-7} \text{ W}$  with each additional light

#### Average Hospital room: 150ft<sup>2</sup>

- average hospital bed size: (38 by 84") (96.52 x 213.36cm) pit bed in center of room, longest distance from wall to bed side:  $415.63/2 = 207.815$

- shortest bed length dimension: 11ft by 13.63ft (335.28cm by 415.63cm)  $\rightarrow 207.815 - (96.32/2)$

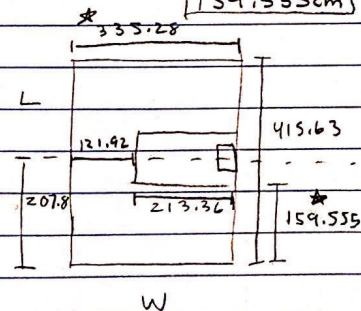
- For square room 12.24ft each way (373.075cm)

#### Longest distances (w/ 1 light)

$$E_k^{vert} = \frac{89.75 \times 10^{-6} \text{ W/cm}^2}{(335.28)^{1.06}} = 1.89 \times 10^{-7} \text{ W wall to wall width}$$

$$E_k^{vert} = \frac{89.75 \times 10^{-6} \text{ W/cm}^2}{(159.555)^{1.06}} = 4.15 \times 10^{-7} \text{ W wall to bed length}$$

★ justifies having 2 lights on all nonfrontal facing sides



## Appendix D

Time of Disinfection:

- at 2m  $500 \mu\text{W}/\text{cm}^2$  generated - at 1m  $6.8 \times 10^{-7} \text{ J/s}$  generated
- $20 \times 10^{-3} \text{ J}/\text{cm}^2$  required to be clean

For  $1 \text{ cm}^2$  to be cleaned:

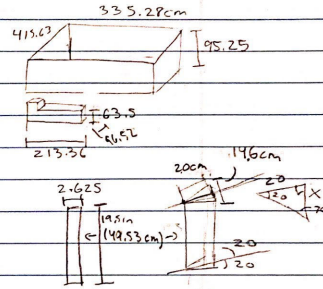
Energy needed to be clean / Energy from 1 light:

$$20 \times 10^{-3} \text{ J}/\text{cm}^2 / 500 \mu\text{W}/\text{cm}^2 = 40 \text{ sec}$$

$$\text{Wall SA: } 2(415.63)(95.25) + 2(335.28)(95.25) = 145,542 \text{ cm}^2$$

$$\text{Ded SA: } 2(213.39)(63.5) + 2(96.52)(63.5) = 39,354 \text{ cm}^2$$

$$\text{Total App SA: } 145,542 + 39,354 = 184,896.895 \text{ cm}^2$$



Angles  $> 20^\circ$  from 0 vastly ↓ energy

- Geometry:

$$\tan(20) = \frac{x}{20} \quad x = 7.28 \text{ cm}$$

$$1 \text{ light hits } \sim (14.6 \times 49.53 \text{ cm}) = 721.097 \text{ cm}^2$$

For  $1 \text{ cm}^2$  to be cleaned by 1 light:

(Total SA / Light SA)  $\times$  (time to disinfect)

$$(184,896.895 \text{ cm}^2 / 721.1 \text{ cm}^2) \times (40 \text{ sec}) = 10,256 \text{ sec} \left( \frac{1 \text{ min}}{60 \text{ sec}} \right) \left( \frac{1 \text{ hr}}{60 \text{ min}} \right) = 2.85 \text{ hr}$$

For  $1 \text{ cm}^2$  to be cleaned by 4 lights:

$$(184,896.895 \text{ cm}^2 / (4 \times 721.1 \text{ cm}^2)) \times (40 \text{ sec}) = 2,564 \text{ sec} \left( \frac{1 \text{ min}}{60 \text{ sec}} \right) = 42.73 \text{ min}$$

Assuming - no light emitted past  $20^\circ$

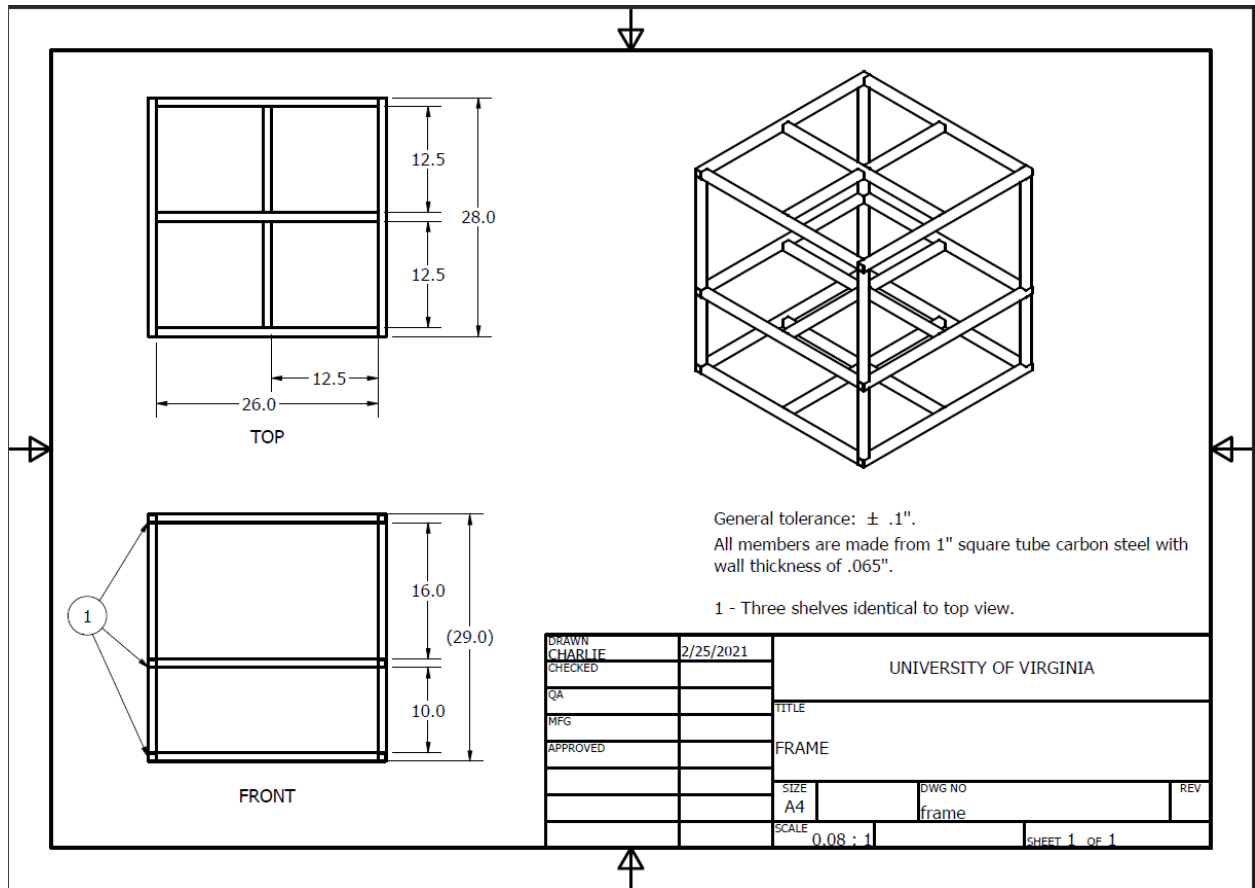
- all lights hit same area

- no other lights on

- room has only 2 lights to disinfect

Scanned with CamScanner

# Appendix E



## Appendix E - MatLab Light Validation Code

```

%% Theoretical Calculations for Lights
LumInt = 89.75*10^(-6); % Theoretical Luminous Intensity value 19.5in
LumIntSpot = 16.73*10^(-6); % Theoretical Luminous Intensity value 12in
L_th=[10 20 30 40 50 60 70 80 90 100]; %cm (.2m=20cm)
L_thB=[207.815 230 260 290 320 350 380 415.63]; %cm (largest dimension 415.63cm) (207 is
length to bed in center of room)

E_Back = (((LumIntSpot)./(L_thB.^1.27))+(.666.*(LumIntSpot)./(L_thB.^1.27))) .*10^6; %W
E_Front = (4.*(LumInt)./(L_th.^1.06)).*10^6; %W
E_Sides = ((2.*(LumInt)./(L_th.^1.06))+(.666.*(LumIntSpot)./(L_th.^1.27))).*10^6; %W
E_SpotLight = ((LumInt)./(L_th.^1.06)).*10^6; %W
OneLight = ((LumInt)./(L_th.^1.06)).*10^6; %W for comparison

%% Experimental Results Back
Dosage_Back_E = [.008 .006 .005 .005 .005 .004 .004 .003]*1000;

%% Experimental Results Front (mW/cm^2)
Dosage_Front_E = [2.23 1.70 1.421 1.035 .694 .620 .497 .334 .265 .197]*1000;

%% Experimental Results Sides
Dosage_Sides_E = [.738 .693 .537 .5 .481 .348 .273 .224 .180 .151]*1000;

%% Graph Theoretical vs. Experimental
AdjustedAxisB = L_thB./100; %cm to m
AdjustedAxis = L_th./100; %cm to m
Dosage_Front = E_Front*100;
Dosage_Back = E_Back*100;
Dosage_Sides = E_Sides*100;
Dosage_SpotLight = E_SpotLight*100;
Dosage_OneLight = OneLight*100; %for comparison

% For Back Panel:
figure (1)
plot(AdjustedAxisB,Dosage_Back,'b--*',AdjustedAxisB,Dosage_Back_E,'r--o') %sides
%plot(AdjustedAxis,Dosage_SpotLight,'b--*') %arm
legend('Theoretical Curve','Experimental Data')
%legend('Back','Front','Sides')
xlabel('Distance (m)')

```

```

ylabel('Dosage (\mu W/cm^2)')
title('Theoretical Versus Experimental Dosages for Back Panel')
%title('Theoretical Dosages at Different Distances for Arm')
hold on

%Front Panel:
figure (2)
plot(AdjustedAxis,Dosage_Front,'b--*',AdjustedAxis,Dosage_Front_E,'r--o',AdjustedAxis,Dosage_OneLight,'g--x')
legend('Theoretical Curve','Experimental Data','One Light')
xlabel('Distance (m)')
ylabel('Dosage (\mu W/cm^2)')
title('Theoretical Versus Experimental Dosages for Front Panel')
hold on

%Side Panels:
figure (3)
plot(AdjustedAxis,Dosage_Sides,'b--*',AdjustedAxis,Dosage_Sides_E,'r--o')
legend('Theoretical Curve','Experimental Data')
xlabel('Distance (m)')
ylabel('Dosage (\mu W/cm^2)')
title('Theoretical Versus Experimental Dosages for Side Panels')
hold on

```

## Appendix F

### Power Calculations

#### Power Consumption of Each Electronic Component

\* assuming everything is running at full capacity

Computer System:  $400 \text{ W}$

UV lights: 1) 19": Quantity = 10  $25 \text{ W}(10) = 250 \text{ W}$   
 2) 9 x 1.375": Quantity = 3  $+ 4 \text{ W}(3) = 12 \text{ W}$   
 3) 12": Quantity = 1  $+ 6 \text{ W}(1) = 6 \text{ W}$   
 $= 268 \text{ W}$

URS Arm:  $390 \text{ W}$

Motor Controllers = Quantity = 4  $\times \frac{20 \text{ A}}{12 \text{ VDC}}$   
 $240 \text{ W} \times 4 \text{ controllers} = 960 \text{ W}$

Emergency Stop Button Receiver:  $25.9 \text{ V}$   
 $\times 45 \text{ mA}$   
 $1.1655 \text{ W}$

DC Fans: 12 V (D.C.) Quantity: 6  
 (12 VDC, 1.5 A)  $12 \text{ V} (1.5 \text{ A})$   
 $\times 6$   
 $10.8 \text{ W}$

LiDAR: 14-20 W power draw  $\Rightarrow 20 \text{ W}$

Total Power Consumption of entire system:  $400 \text{ W} + 268 \text{ W} + 960 \text{ W} + 1.1655 \text{ W} + 10.8 \text{ W} + 390 \text{ W} + 20 \text{ W} =$   
 $= 2,049.9655 \text{ W}$

Current from battery  $= 2,049.9655 \text{ W} / 25.9 \text{ V} =$   
 $79.15 \text{ amps} \Rightarrow 10 \text{ avg}$

### DC-AC converter wire calculation:

$$\begin{array}{r} 268 \text{ W} - \text{lights} \\ + 20 \text{ W} - \text{LiDAR} \\ 390 \text{ W} - \text{arm} \\ 400 \text{ W} - \text{computer} \\ \hline 1,078 \text{ W} \end{array}$$

$$1,078 \text{ W} / 25.9 \text{ V} = 41.62 \text{ amps}$$



10 awg wire for DC/AC converter

### DC-DC step down converter wire calculation:

$$\begin{array}{r} + 960 \text{ W} - \text{motor controllers} \\ + 1.1655 \text{ W} - \text{e-stop receiver} \\ + 10.8 \text{ W} - \text{fans} \\ \hline 971.97 \text{ W} \end{array}$$

$$971.97 \text{ W} / 25.9 \text{ V} = 37.82 \text{ amps}$$



10 awg wire

22,000 mAh 25.9 V batteries in parallel  
yields 44,000 mAh battery system

(mAh = milli amp hour)

$$\frac{44,000 \text{ mAh}}{.53 \text{ hr}} \times \text{amps } (25.9 \text{ V}) = 2,150.19 \text{ W}$$

• 53 hr = 32 minutes run time @ full capacity

# Appendix G

Amperes	250-300	4-ga.	2-ga.	2-ga.	1/0-ga.	1/0-ga.	1/0-ga.	2/0-ga.
	200-250	4-ga.	4-ga.	2-ga.	2-ga.	1/0-ga.	1/0-ga.	1/0-ga.
	150-200	6 or 4-ga.	4-ga.	4-ga.	2-ga.	2-ga.	1/0-ga.	1/0-ga.
	125-150	8-ga.	6 or 4-ga.	4-ga.	4-ga.	2-ga.	2-ga.	2-ga.
	105-125	8-ga.	8-ga.	6 or 4-ga.	4-ga.	4-ga.	4-ga.	2-ga.
	85-105	8-ga.	8-ga.	6 or 4-ga.	4-ga.	4-ga.	4-ga.	4-ga.
	65-85	10-ga.	8-ga.	8-ga.	6 or 4-ga.	4-ga.	4-ga.	4-ga.
	50-65	10-ga.	10-ga.	8-ga.	8-ga.	6 or 4-ga.	6 or 4-ga.	4-ga.
	35-50	10-ga.	10-ga.	10-ga.	8-ga.	8-ga.	8-ga.	6 or 4-ga.
	20-35	12-ga.	10-ga.	10-ga.	10-ga.	10-ga.	8-ga.	8-ga.
	0-20	12-ga.	12-ga.	12-ga.	12-ga.	10-ga.	10-ga.	10-ga.
		0-4 ft.	4-7 ft.	7-10 ft.	10-13 ft.	13-16 ft.	16-19 ft.	19-22
Length in feet								